Soft Matter

PAPER

View Article Online
View Journal | View Issue

Cite this: *Soft Matter*, 2021, **17**, 8130

Surface alignment of ferroelectric nematic liquid crystals†

Federico Caimi,[a] Giovanni Nava,[a] Raouf Barboza,[b] Noel A. Clark,[c] Eva Korblova,[d] David M. Walba,[d] Tommaso Bellini*[a] and Liana Lucchetti*[b]

Received 18th May 2021,
Accepted 9th August 2021

DOI: 10.1039/d1sm00734c

rsc.li/soft-matter-journal

The success of nematic liquid crystals in displays and optical applications is due to the combination of their optical uniaxiality, fluidity, elasticity, responsiveness to electric fields and controllable coupling of the molecular orientation at the interface with solid surfaces. The discovery of a polar nematic phase opens new possibilities for liquid crystal-based applications, but also requires a new study of how this phase couples with surfaces. Here we explore the surface alignment of the ferroelectric nematic phase by testing different rubbed and unrubbed substrates that differ in coupling strength and anchoring orientation and find a variety of behaviors – in terms of nematic orientation, topological defects and electric field response – that are specific to the ferroelectric nematic phase and can be understood as a consequence of the polar symmetry breaking. In particular, we show that by using rubbed polymer surfaces it is easy to produce cells with a planar polar preferential alignment and that cell electrostatics (*e.g.* grounding the electrodes) has a remarkable effect on the overall homogeneity of the ferroelectric ordering.

Introduction

A nematic (N) liquid crystal (LC) is a fluid of structurally anisotropic molecules in which there is a local tendency for coherent orientation that is strong enough to produce long-range order. This ordering is manifested by elastic energy associated with spatial gradients of the orientation field. Elasticity stabilizes spatial uniformity in the absence of external forces and makes the nematic macroscopically collective so that, in the absence of constraints, an arbitrarily small applied electric or magnetic field can orient a bulk nematic sample by coupling to nematic orientation *via* quadrupolar anisotropy. The N order is similarly highly responsive to boundary conditions, *i.e.*, to surfaces favouring a specific molecular orientation. Because the N is a fluid, these conditions make it in principle possible to put it in a container with patterned surfaces, and have it spontaneously adopt a designed, space-filling, three-dimensional (3D) orientational structure. Technologies based on N LCs exploit the competition between high responsivity to fields and boundary conditions by which surface-induced 3D structures respond in a predictable way to applied fields. Any new application exploiting N ordering equally rests on understanding and controlling surface and field interactions.

A novel LC phase[1–4] has recently been shown to be a ferroelectric nematic (N_F), that is a 3D liquid having a macroscopic electric polarization $\boldsymbol{P}(\boldsymbol{r})$.[5] In this new phase each molecular dipole is nearly parallel to its molecular steric long axis, a condition which macroscopically translates into a strong orientational coupling making $\boldsymbol{P}(\boldsymbol{r})$ locally parallel to $\pm\boldsymbol{n}(\boldsymbol{r})$, the nematic director, *i.e.* the unit vector defining the average quadrupolar molecular orientation. The self-stabilized spontaneous polar ordering of N_F is nearly complete 3,5, with a polar order parameter, $p = \langle\cos(\beta_i)\rangle \gtrsim 0.9$, where β_i is the angle between each molecular dipole and the local average $\boldsymbol{P}$ direction. The resulting spontaneous polarization is remarkably large, $P \sim 6\ \mu C\ cm^{-2}$, enabling a linear coupling between $\boldsymbol{n}(\boldsymbol{r})$ and external electric fields $\boldsymbol{E}$, not present in conventional nematics. Such polar linear coupling is, at low $\boldsymbol{E}$, much larger than the dielectric quadrupolar coupling of N LCs, with an associated electro-optic response to fields as small as $\sim 1\ V\ cm^{-1}$, a thousand times smaller than those used to reorient dielectric nematics. This extremely large responsivity offers a variety of opportunities to employ applied fields and surface phenomena in new ways.

Here we explore the surface alignment of the N_F phase induced by various rubbed and unrubbed substrates.

[a] *Medical Biotechnology and Translational Medicine Dept., University of Milano, 20054 Segrate, Italy. E-mail: tommaso.bellini@unimi.it*
[b] *Dipartimento SIMAU, Università Politecnica delle Marche, via Brecce Bianche, 60131 Ancona, Italy. E-mail: l.lucchetti@univpm.it*
[c] *Department of Physics, Soft Materials Research Center, University of Colorado, Boulder, CO, 80305, USA*
[d] *Department of Chemistry, Soft Materials Research Center, University of Colorado, Boulder, CO, 80305, USA*

† Electronic supplementary information (ESI) available. See DOI: 10.1039/d1sm00734c

We observe that confining surfaces have a strong influence on the formation of different orientational patterns and domains[6] and show that the polar ordering appearing at the N–N_F phase transition changes the interactions of the director with bounding surfaces, a key aspect of nematic LC science and its potential for technology. We demonstrate that by designing the polarity of the 2D bounding surfaces, it is possible to control the 3D structuring of $\boldsymbol{P}(\boldsymbol{r})$ in the N_F phase. In the simplest example, if the orientation of the preferred polarization is vectorially unidirectional on the confining surfaces, then the N_F volume polarization can be similarly oriented, that is, poled into a uniform orientation by the surfaces without the need for an applied field.[7]

Materials and methods

The ferroelectric liquid crystal 4-[(4-nitrophenoxy)carbonyl] phenyl2,4-dimethoxybenzoate RM734 was synthesized as reported in ref. 5. Its structure and phase diagram are shown in Fig. 1a and c. RM734 was loaded by capillarity in the N phase into thin cells (Fig. 1b) formed by two flat plates held by spacers at a distance d = 10 μm or d = 18 μm depending on the cell construction. Most of the cells are equipped with aluminium or ITO electrodes enabling the application of in-plane electric fields, with inter-electrode distance ranging from 2 to 5 mm. The three possible electrodes configurations used in the experiments are reported in Fig. 1b: (i) floating, (ii) connected to ground, (iii) connected to a function generator.

We prepared several different cells by surface treating the plates, some of which were rubbed, *i.e.* mechanically brushed in one direction. Four vectorial directions are relevant to describe the cells and their behavior (Fig. 1b): the rubbing direction ($\boldsymbol{R}$, unit vector $\mathbf{u}_R$), the electric field direction ($\boldsymbol{E}$, $\mathbf{u}_E$), the polarization direction ($\boldsymbol{P}$, $\mathbf{u}_P$) and the loading direction ($\boldsymbol{F}$, $\mathbf{u}_F$), providing the direction of the shear flow when the cell is loaded. Cells with rubbed substrates were assembled with equal $\boldsymbol{u}_R$ on both sides.

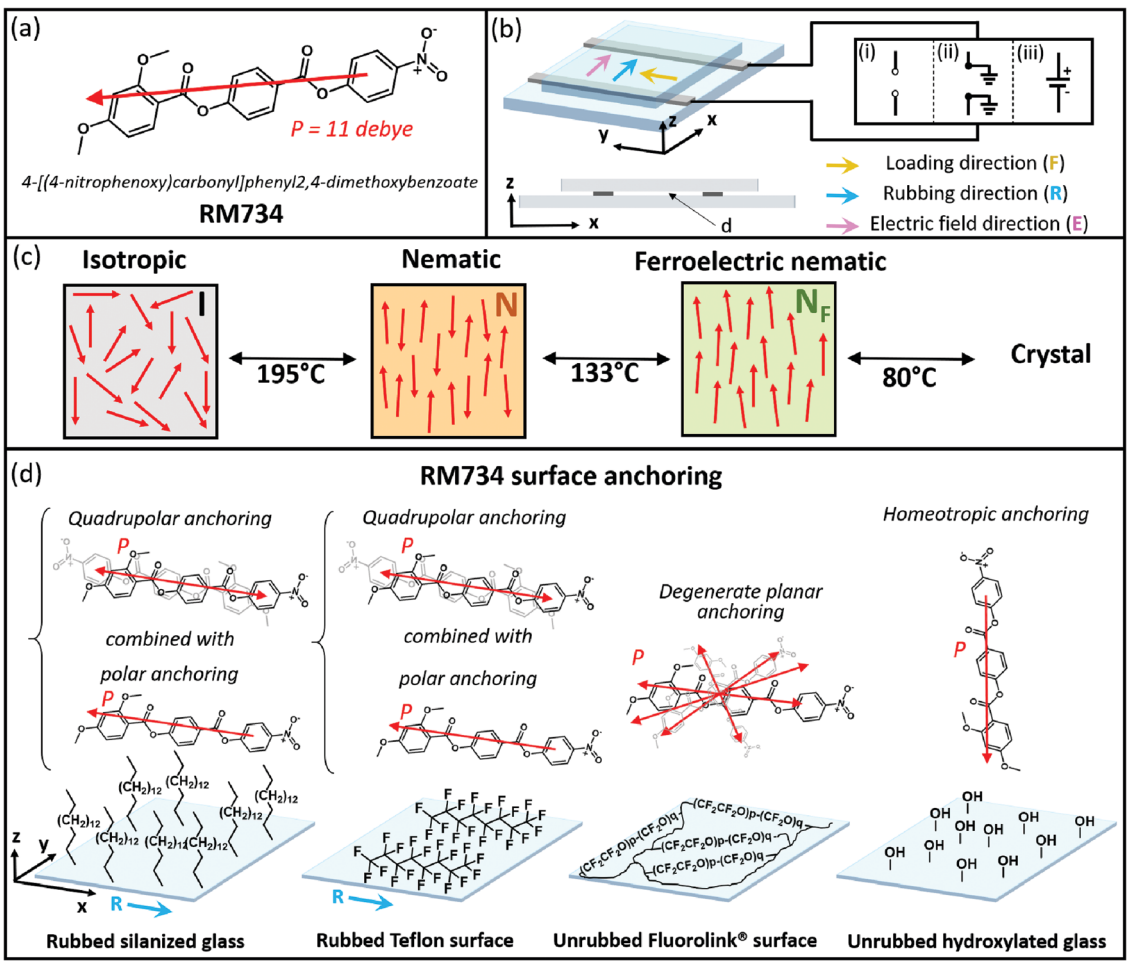

Fig. 1 Liquid crystal cells. (a) Molecular structure of RM734 and orientation and strength of the molecular dipole. (b) RM734 was loaded into thin cells formed by two planar slabs held at a distance d by spacers and provided of electrodes. In the figure we introduce the coordinates and the relevant directions (***F, R, E***) that we use to describe the results and the three electrodes configurations used in the experiments: (i) floating, (ii) connected to ground, (iii) connected to a function generator (c) sketches of the three phases and transition temperatures. (d) Sketches of the four surfaces studied in this work and of the orientation of the RM734 molecules with respect to the substrates.

In this work we considered four different surfaces, whose preparation is detailed in the ESI:†

(i) Rubbed silanized surfaces: glass coated with aliphatic C16 chains grafted *via* a terminal reactive silane group. Rubbing was provided by gentle brushing with a soft tissue.

(ii) Rubbed *Teflon* surfaces: glass plates were rubbed with a heated polytetrafluoroethylene (PTFE) rod while exerting pressure;

(iii) Unrubbed *Fluorolink* surfaces: spin-coated perfluoropolyether urethane methacrylate (Solvay Fluorolink MD700) provides a cross-linked fluorinated polymer network on the glass surface;

(iv) Unrubbed hydroxylated glass surfaces, obtained by treating glass plates with piranha solution.

Cells were characterized by observations at Polarized Transmission Optical Microscopy (PTOM) at various temperatures (T), and in particular in the N phase at $T = 180\ ^\circ$C and in the N_F phase at $T = 130\ ^\circ$C. Movies showing the transitions between the two phases, by continuously changing T, are available in ESI.† Birefringence measurements performed on planar cells yield $\Delta n = 0.20$ in N phase at $T = 180\ ^\circ$C and $\Delta n = 0.23$ in the N_F phase at $T = 130\ ^\circ$C. In most cases, N_F phase was obtained by cooling the cells from the N phase with unconnected (floating) electrodes, a procedure that we refer to as ''Zero Field Cooling'' (ZFC). The electric field response of N_F was studied in two ways: by applying the field to the ZFC cells and by applying the field in the N phase and cooling the system into the N_F phase by keeping the field on across the transition (Field Cooling, FC). The FC procedure is meant to investigate if the polar coupling with the N_F pretransitional fluctuations – at the same time responsive and free to rotate – influences the surface anchoring as the N_F ordering extends throughout the cell.

Experimental results

We find that both the texture of the N_F phase and its response to in-plane fields depend on the kind of confining surfaces used to build the cell. Most of the behavior that we report here is a consequence of the lower symmetry of N_F with respect to N, by which ordering with same $\boldsymbol{n}$ might have different p, a condition that leads to the formation of topological defects and domain walls not observed in conventional N. The reduced symmetry has a relevant effect in the coupling with the surfaces since, on top of the quadrupolar coupling with $\boldsymbol{n}$, we find an additional polar anchoring whose strength depends on the substrate and its treatment, as summarized in Fig. 1d for the four substrates. Indeed, while unrubbed Fluorolink constrain the N_F phase of RM734 to be parallel to the substrates, and thus with no polar coupling, rubbed Teflon provides instead a strong quadrupolar planar anchoring ($\boldsymbol{n} = \pm\boldsymbol{u}_R$) combined with a rather strong polar planar coupling (surface $\boldsymbol{u}_P = -\boldsymbol{u}_R$). In between these surface couplings is the rubbed silanized glass, which also shows strong quadrupolar planar anchoring, but with a less relevant polar coupling.

The effects of broken symmetry and appearance of electric polarization become particularly evident at the N–N_F transition, where dramatic texture transformations and sudden appearance of topological defects are observed in all the cells we have examined. Particularly evident is the effect of N–N_F transition on unrubbed hydroxylated glass since it implies a conversion from homeotropic (non-polar) anchoring in the N phase to random planar (polar) coupling in the N_F phase.

Cells with substrates made by rubbed C16 silanized glass

Silane-coated surfaces, known to generally induce homeotropic ordering of thermotropic nematics,[8] favour instead the planar alignment of RM734, which can be oriented in any direction by gentle surface rubbing. Fig. 2 shows PTOM pictures demonstrating that the N phase exhibits a good homogeneous planar alignment in the direction of rubbing, both right after cell filling (Fig. 2a) and when the N phase is obtained on heating from the N_F phase (Fig. 2b). Upon ZFC to the N_F phase, several domains appear while the overall homogeneous alignment is retained (Fig. 2c and video S1, ESI†). These domains are twisted regions connecting surfaces of reversed polarity, as it is revealed by tilting the analyzer clockwise (lower left panel) and counter-clockwise (lower right panel), revealing regions where the N–N_F transition leads to a surface polarity which is parallel to rubbing but with a reversed direction. This indicates that the unidirectional rubbing of silane-coated surfaces leads to quadrupolar in plane alignment strong enough to be maintained on all the surface, and to weaker polar surface coupling, which is occasionally reverted. Sketches of the molecular alignment across the cell in different regions marked by Greek letters are reported in Fig. 2d. Regions α and δ are uniformly aligned in opposite directions, while β and γ are twisted (with either right or left-handed rotation) because one surface or the other has reversed polarity. The nearly identical polarization state of the light transmitted by the uniform and twisted regions is due to a good adiabatic rotation which is expected given the large birefringence and the cell thickness, as also demonstrated by the different behaviour of equal but thinner cells (Fig. S1 of the ESI†) where the twist is tighter and the rotation incomplete. The reason behind the existence of areas with reversed surface polarity is revealed by video S1 (ESI†) which shows the development of the polar domains that form during the ZFC N–N_F phase transition and lead to the texture observed in Fig. 2c. As T is lowered, the N_F phase appears locally in multiple locations in the cell. When these come into contact with the surfaces, the surface polarity is locally locked by the quadrupolar anchoring. When such locked polarity is opposite on two facing surfaces, a twisted structure is formed. However, twisted domains are found on only a fraction of the surface, indicating that the polar order on the surface has a preferential direction, and thus that the surface is exerting a polar coupling with the ferroelectric order parameter p. Since the contact between twisted and uniform domains involves both an elastic penalty – because of the director distortion – and an electrostatic penalty – because of the accumulation of polarization charges –, the stability of the twisted domains is rather intriguing. A crucial clue to answer this question is revealed by the sudden disappearance of the twisted domains

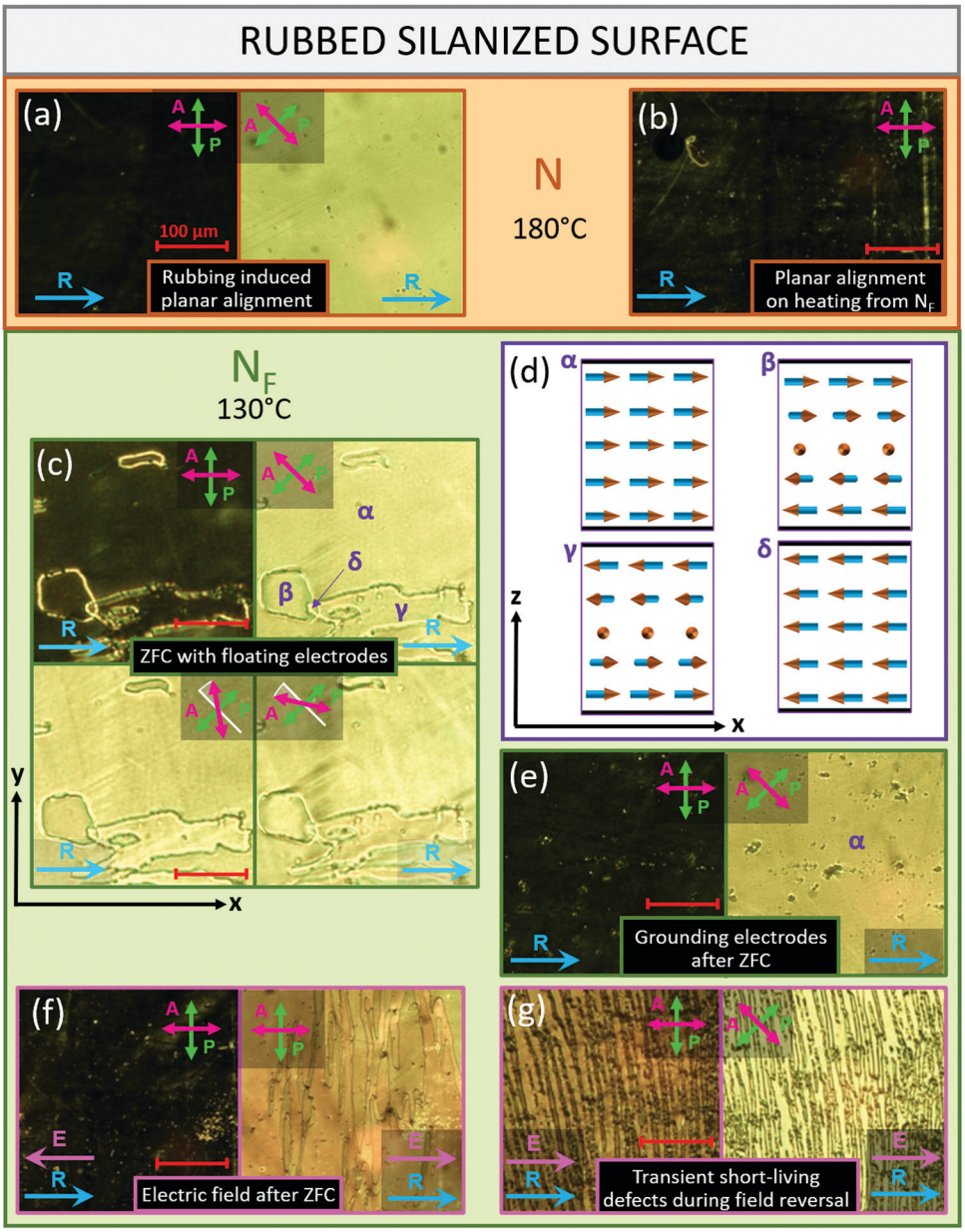

Fig. 2 Polarized transmission optical microscopy images of 18 µm thick RM734-filled cells having rubbed C16 silanized surfaces. Arrows: rubbing direction (***R***), analyzer (***A***), polarizer (***P***), electric field (***E***). Shadings: nematic phase (orange), ferroelectric nematic phase (green). (a) Cells filled in N phase exhibit planar alignment. (b) Planar alignment is also found after heating from the N_F phase. (c) On zero-field cooling (ZFC) from N phase the planar alignment is maintained except for domains where the surface polarity is reversed (upper panels). Opposite surface polarity induces a twist pattern, as revealed by rotating the analyzer clockwise (lower left panel) and counter-clockwise (lower right panel). (d) Sketches of the alignment across the cell (*xz* cut) of the domains marked by α-δ letters. Domains observed on cooling with floating electrodes (c) disappear when the electrodes are grounded (e). Electric field effects on N_F phase (pink frames). (f), left panel: applying a 1 V cm^{-1} field opposite to ***R*** ($\boldsymbol{u}_E = -\boldsymbol{u}_R$), the N_F phase is stabilized and twisted domains disappears. Right panel: As the same field is applied along ***R*** ($\boldsymbol{u}_E = \boldsymbol{u}_R$) a twisted state is induced. (g) Transient short living defect lines appear right after inverting the field. The value of the scale bar is indicated in the first panel.

that follows connecting the electrodes to ground (Fig. 2e). Indeed, the electric field generated by the surface charge that accumulates in the N_F phase at the RM734-electrodes interfaces – on the *yz* plane, perpendicular to $\boldsymbol{u}_R$ – is opposite to $\boldsymbol{u}_P$, thus greatly reducing, if not reversing, the tendency toward uniform ferroelectric alignment. Such a counter-field is cancelled by connecting the electrodes to ground since this allows the flow of free charges toward the interface to compensate the polarization charges.

The existence of a surface polar coupling on top of the quadrupolar anchoring becomes clear by studying the response of ZFC N_F to the application of electric fields in the direction of rubbing. Such response, shown in video S2 (ESI†) and Fig. 2f, is markedly asymmetric: a field E = 1 V cm^{-1} antiparallel to rubbing ($\boldsymbol{u}_E = -\boldsymbol{u}_R$) cancels the domains and stabilizes the alignment, while the same field in the parallel direction ($\boldsymbol{u}_E = \boldsymbol{u}_R$) is not enough to revert the polarity, producing instead a

twisted texture. Polarity reversal, yielding a uniform alignment in the $\boldsymbol{u}_E = \boldsymbol{u}_R$, can only be obtained with larger fields, $E > 5$ V cm^{-1}.

Fig. 2g shows the pattern of defect lines developing right after the field reversal, indicating that, in the presence of an opposing field, the N_F alignment breaks into stripe-shaped domains perpendicular to the field, in line with previous observations.[5] The time evolution of these domains (shown in video S2, ESI†) leads to a double system of topological lines that are at different heights in the cell and thus move without intersecting, giving rise to textures as in Fig. 2f, right-hand side panel, whose structure is analyzed in Fig. S2 (ESI†). Fig. S2 (ESI†) (frame VI) also shows a clean example of reversed surface polarity, supporting the notion of strong quadrupolar and weak polar anchoring.

Cell textures observed upon field cooling are similar to those obtained by applying a field on ZFC N_F. In both ZFC and FC cells, the alignment induced by the electric field is not stable upon field removal as we observe the reappearance of polar domains as those in Fig. 2c.

Cells with Teflon-rubbed substrates

Teflon-rubbed plates also favours the planar alignment of RM734 molecules, a behaviour this time common to other LC compounds.[9,10] Analogously to rubbed silane, the surface exhibits a quadrupolar coupling with the N ordering and planar alignment of the N_F phase antiparallel to rubbing ($\boldsymbol{u}_P = -\boldsymbol{u}_R$), although with some significant difference.

Fig. 3a shows the homogenous planar alignment along the rubbing direction observed after loading a 10 μm thick cell in the N phase. The alignment is independent on the loading direction. Upon ZFC RM734 into the N_F phase, several domains appear within an overall homogeneous aligned cell (Fig. 3c and video S3, ESI†). As in the case of silanized glasses, these are twisted polar domains connecting antiparallel surface polarizations on the two confining plates, corresponding to regions on either of the surfaces where the surface polarity reverses. The difference in brightness between twist domains and uniform background is due to an imperfect adiabatic rotation because of the small cell thickness in analogy to silanized cells discussed in the ESI† (Fig. S1). Domains are delimited by thin bright lines that become dark upon 45° rotation of the polarizers (Fig. 3c and d). These lines correspond to a twist-bend deformation connecting the twisted LC inside the domains to the untwisted LC outside them as sketched in Fig. 3e. A fraction of the domains also shows an internal defect line, as in the case in Fig. 3d, that we understand as a defect line separating two regions of opposite twist, as sketched in Fig. 3f. As T is raised into the N phase, a few of such domains remain pinned on the surface (Fig. 3b). Their darker appearance with respect to those observed in the lower temperature phase is probably due to the lower birefringence of the N phase[5] that reduces the adiabatic rotation.

The effect of the application of an in plane electric field is observable in the pink frames of Fig. 3. The brightness variation observed with a field $E = 1$ V cm^{-1} antiparallel to rubbing ($\boldsymbol{u}_E = -\boldsymbol{u}_R$) indicates that the uniform background is unaffected, while in the twist domains $\boldsymbol{n}$ undergoes partial in-plane reorientation that effectively narrows the twisted region within the cell. This reduces the adiabatic rotation thus resulting in a larger transmitted light. When the same field is applied parallel to rubbing ($\boldsymbol{u}_E = \boldsymbol{u}_R$), LC reorientation is observed mainly outside the twisted domains. Here the electric field induces a twisted state in the previously uniform regions, being insufficient to reverse the polarity.

When field cooled with $\boldsymbol{u}_E = -\boldsymbol{u}_R$, the behavior of the cell is different: small domains are suppressed, resulting in a generally uniform ferroelectric phase aligned with $\boldsymbol{n}$ along rubbing ($\boldsymbol{u}_P = -\boldsymbol{u}_R$). For large enough fields ($E \geq 1$ V cm^{-1}), the cell becomes fully aligned (Fig. 3h, left panel and video S4, ESI†). This FC alignment is maintained after field removal (Fig. 3i) in both $d = 10$ μm and $d = 18$ μm cells. The difference between FC and ZFC, *i.e.* the fact that portions of the surfaces can hold orientations with opposite polarity, indicates that the quadrupolar directional coupling, always observed throughout the whole cells, is stronger than the polar coupling, which depends on the cell history. When the cell is instead field-cooled with $\boldsymbol{u}_E = \boldsymbol{u}_R$, it is broken into a variety of domains showing three levels of brightness, corresponding to the following three situations: (i) the polarity on both surfaces is equal to the field direction and the cell is uniformly oriented (black); (ii) the polarity on the two substrates is in opposite directions, which produces a twisted structure compressed against the surface where the polarity is opposite to the field. In this case the twist is too tight to produce adiabatic rotation, so that the outcoming light is elliptically polarized with a partially rotated axis, giving rise to partial brightness; (iii) the polarity on both substrates is opposite to the field giving rise to two π twisted regions compressed against the two surfaces, leading to a polarization state that is difficult to evaluate, but is, quite reasonably, more deformed from linearity, and thus brighter, than in the previous case (Fig. 3h, right panel and Fig. S3, ESI†). Overall, evidence on rubbed Teflon surfaces indicate that the anchoring induced by this treatment, besides the quadrupolar coupling, contains a significant polar term where the preferred polarity is $\boldsymbol{u}_P = -\boldsymbol{u}_R$, as in rubbed silane, as it appears from: (i) the asymmetric field response, with high threshold for FC $\boldsymbol{u}_p = \boldsymbol{u}_R$ field alignment, which is not observed for fields up to $E = 10$ V cm^{-1}; (ii) the persistence of domains when heating the cell from N_F to N phase; (iii) the different texture of the N_F phase upon FC and ZFC. Evidence i and ii indicate a polar anchoring stronger than in the case of rubbed silanized glasses.

Cells with substrates made by Fluorolink-coated glass

We explored the behaviour of Fluorolink-coated cells prepared with different loading directions with respect to the direction of $\boldsymbol{E}$ and with both values of cell thickness.

We find that the N phase aligns planarly on this substrate, but with a remarkably weak anchoring direction. As the cell is loaded in the N phase, the loading direction determines the direction of planar alignment, as shown in Fig. 4a, which is homogenous and stable. As the cell is heated in the isotropic

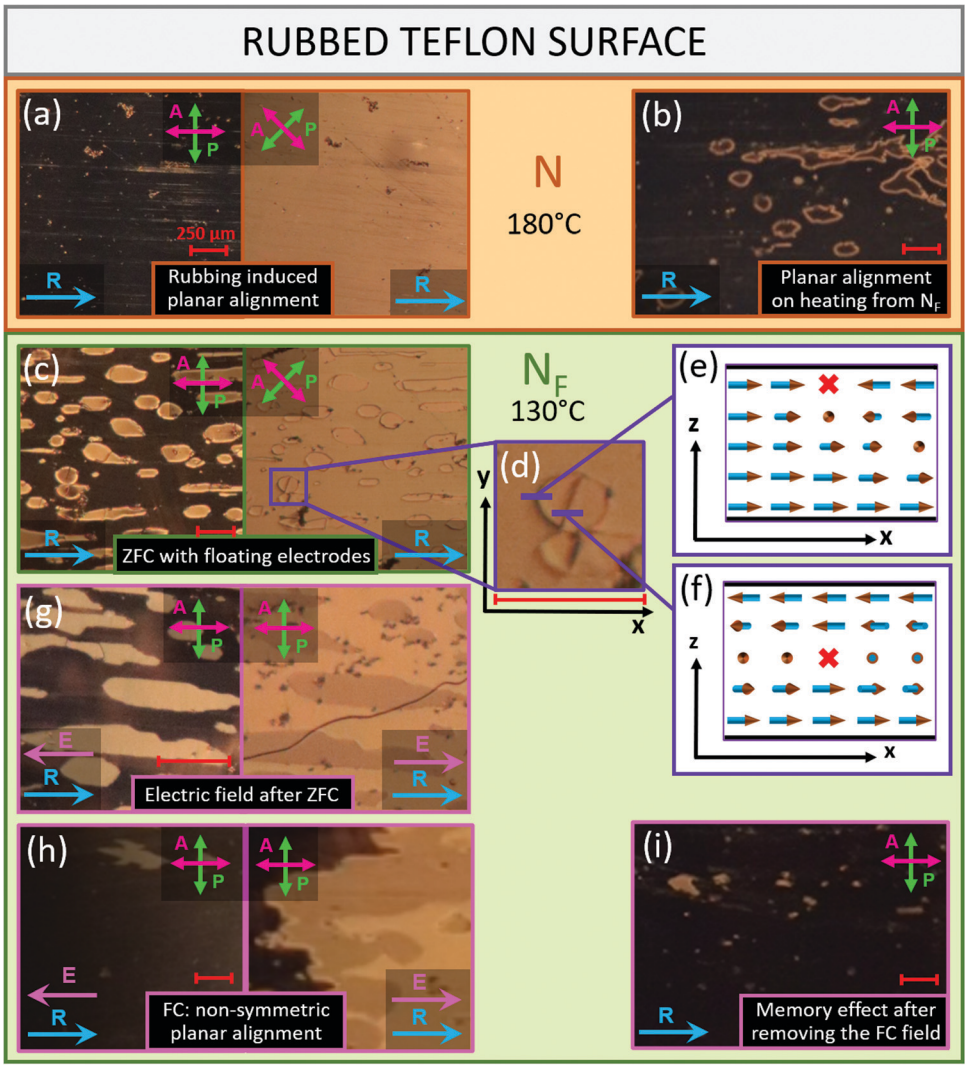

Fig. 3 Polarized transmission optical microscopy images of 10 µm thick RM734-filled cells having rubbed Teflon surfaces. Arrows: rubbing direction (***R***), analyzer (***A***), polarizer (***P***), electric field (***E***). Shadings: nematic phase (orange), ferroelectric nematic phase (green). (a) Cells filled in N phase exhibit planar alignment. (b) Alignment after heating from the N_F phase is planar with remnant twist domains. (c) Polar planar alignment (dark background in the right-handed panel) is disrupted by twisted domains due to reversed polar anchoring. (d) Enlargement of a domain showing contour and internal defect lines, described in panels (e) and (f), respectively. Electric field effects on N_F phase (pink frames). (g) Electric field application reveals strong polar surface anchoring. Electric field effects on N_F phase (pink frames). Left panel: Upon applying an electric field opposite to rubbing ($\boldsymbol{u}_E = -\boldsymbol{u}_R$), the uniform planar background is stabilized, while the twist domains are modified so to reduce the adiabatic rotation and enhance the transmitted light. Right panel: When ***E*** is along ***R*** ($\boldsymbol{u}_E = \boldsymbol{u}_R$), fields up to 10 V cm^{-1} are insufficient to reverse the polarity, inducing a twisted state in the previously uniform dark regions. (h) Left panel: Field-cooling with $E \geq 1$ V cm^{-1} and $\boldsymbol{u}_E = -\boldsymbol{u}_R$ yields uniform alignment, which remains after removing the field (i). (h) Right panel: Field cooling with $E = 1$ V cm^{-1} and $\boldsymbol{u}_E = \boldsymbol{u}_R$ yields textures with domains having three different brightnesses. The value of the scale bar is indicated in the first panel.

phase and cooled back into the N phase, the memory of the loading direction is lost and Schlieren textures are observed (Fig. 4b). The appearance of Schlieren textures with point defects of strength 1/2 and 1 indicates that the planar anchoring is strong enough to prevent dissolving the defects by tilting in the *z*-direction. The formation of Schlieren textures indicates also that the anchoring is planar degenerate. The very fact that any position of the cell can be extinguished (as the black stripes of Fig. 4b) by a suitable rotation between crossed polarizers demonstrates that the nematic ordering is uniform (*i.e.* untwisted) across the cell, in turn indicating that the weak torsional forces developing from nematic director twists are enough to produce rotational sliding on the surfaces.

Upon cooling into the N_F phase from both homogenous planar (Fig. 4a) and Schlieren texture (Fig. 4b), we obtain the defected structures in Fig. 4c and d. In the texture of Fig. 4c the overall alignment is preserved, while the system appears to exploit the weak coupling to slowly surface-slide and rearrange into locally ordered planar regions bounded by defect lines preferentially aligned along the director ***n***. These lines have an elaborate structure featuring double black stripes (Fig. 4c–f). Such defects slowly shrink until they reach a stationary pattern, possibly stabilized by surface imperfections. Analogously, upon

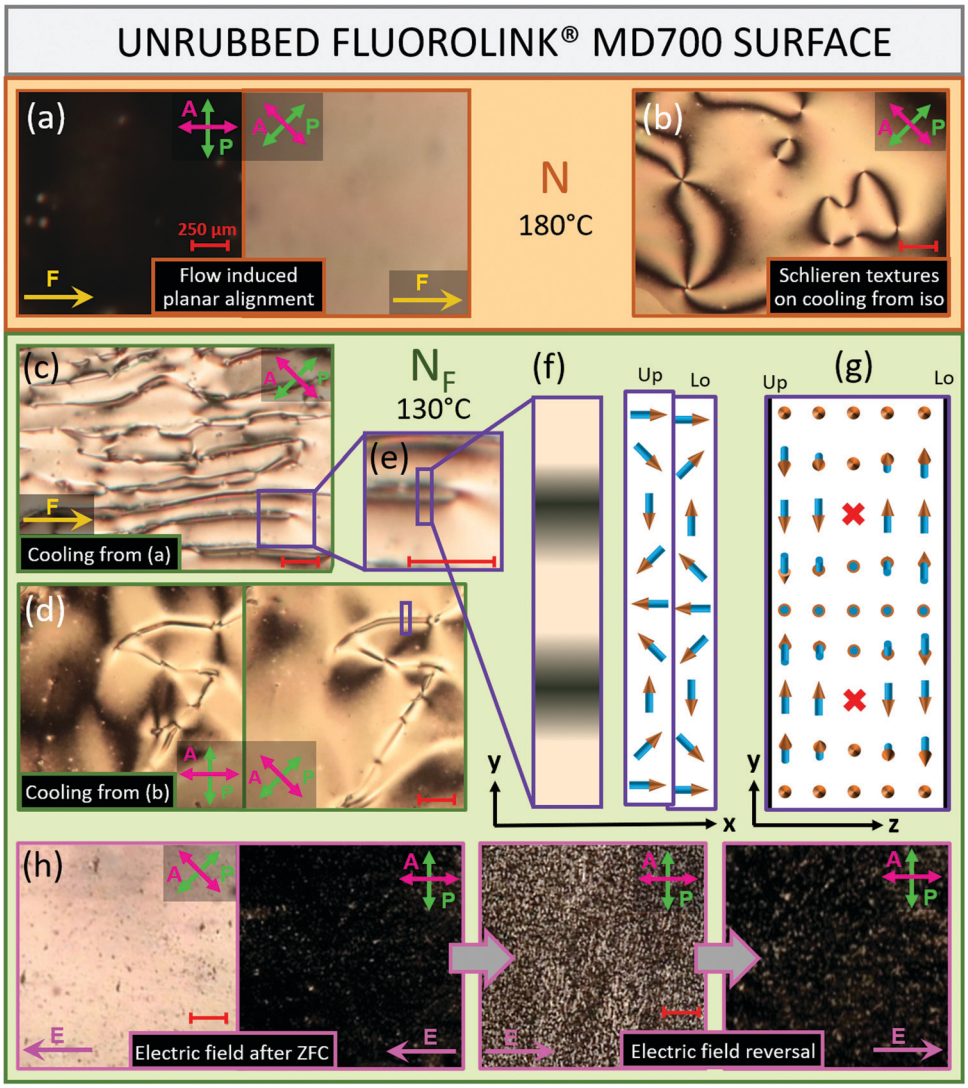

Fig. 4 Polarized transmission optical microscopy images of 18 µm thick RM734-filled cells having unrubbed fluorinated polymer surfaces. Arrows: analyzer (***A***), polarizer (***P***), electric field (***E***), loading flow direction (***F***). Shadings: nematic phase (orange), ferroelectric nematic phase (green). (a) Cells filled in N phase exhibit planar alignment in the loading direction. (b) Upon cooling from the isotropic phase, the N cell shows Schlieren texture. Ferroelectric nematic phase (green shading). (c) and (d) Are obtained by cooling with no field into the N_F phase the cells in (a) and (b) respectively. We interpret the structure of the lines featuring a double dark band (purple frame in panes c and d), as an effect of opposite surface rotation, as sketched in the panels (e)–(g). The polar nature of the N_F phase gives rise in this case to opposite twists separated by topological defects, a configuration that greatly reduces the brightness due to scattering from defects and partial adiabatic rotation. Electric field effects on N_F phase (pink frames). (h) Field induced uniform orientation is obtained in zero-field cooled cells with low fields, $E \geq 0.5$ V cm^{-1} (h – first, second and fourth panel). Right after ***E*** switching, a disordered transient state is observed demonstrating polar response (h – third panel), yielding a fully ordered state (h – fourth panel) with reversed polarity in about 1s. The value of the scale bar is indicated in the first panel.

cooling into the N_F phase the Schlieren texture in Fig. 4b, the system stabilizes on a smooth pattern with similar "two-line" defects (Fig. 4d). We interpret these lines as an effect of the strong planar but degenerate anchoring: upon cooling, as the polar ordering develops, domains with opposite polarity nucleate, connected through a variety of possible π or $-\pi$ director rotation on the surfaces, and a corresponding variety of adiabatic rotation. When such rotations (π or $-\pi$) are opposite on the two cell walls, "trapped" splay-twist distortion lines are created. As the structure anneals and one polarity prevails, such splay-twist lines collapse in pairs to minimize the elastic cost, yielding the structure described in the schemes in Fig. 4f–g. The polar nature of these domains becomes apparent when an in-plane electric field is applied to the cell. Regardless from the direction of filling and the thermal and electric history of the sample, fields as small as $E = \pm 0.5$ V cm^{-1} induce a defect-free alignment of the director along ***E*** (Fig. 4h, first, second and fourth panel). The dramatic rearrangement that follows field inversion (third panel), indicates that the polarity ***P*** follows the field orientation. No difference is observed between FC and ZFC, in agreement with the notion of degenerate (non-polar) surface coupling. The degenerate planar

coupling of this substrate also enables to perform a rough estimate of the origin of the $E = \pm 0.5$ V cm^{-1} threshold. When the N_F is ordered in the direction of $\boldsymbol{E}$, a surface charge density $\sigma = \boldsymbol{P}\cdot\boldsymbol{n} \approx 6$ μC cm^{-2} develops at the electrodes,[5] $\boldsymbol{n}$ being the normal to the electrode–LC interface. In the absence of conduction charges compensating σ at the electrode, this accumulation of charges induces a field opposing the N_F polarity, and possibly stabilizing the antiparallel domain, as discussed above. In the presence of mirror charges of matching surface density σ, the field within the LC vanishes, while two double layers of charges are localized at the two LC-electrode interfaces, corresponding to two potential differences $\Delta V_e = \sigma\delta/\varepsilon$ where ε is the permittivity and δ the width of each double layer. We obtain $\delta \sim 10$ nm, a quantity that appears reasonable, given the roughness of the electrodes and the possible disordering of the first layer of electrode-contacting molecules.

The defect-free texture induced by the electric field is partially lost as the field is removed and a few defect lines reappear. However, grounding the electrodes after field removal enable preserving the field-induced orientation. This is analogous to what observed with the other substrates, again indicating that the presence of compensating charges on the electrodes is crucial to the overall alignment of the N_F phase.

Cells with substrates made by hydroxylated glass

Hydroxylated glass cells exhibit two distinct surface-RM734 coupling in the two nematic phases: uniform homeotropic (*i.e.* perpendicular to substrates) ordering in the N phase (Fig. 5a) and inhomogeneous planar alignment in the N_F phase (Fig. 5b). The homeotropic anchoring in the N phase is stable and is obtained only after heating into the isotropic phase, while right after filling at $T = 180$ °C a random planar texture, similar to the one in Fig. 5b, is observed. Homeotropic anchoring on uncoated glass is atypical for nematic compounds, as the most commonly observed alignment is random planar. However, recent observation on cyano LC compound on plasma-cleaned glasses

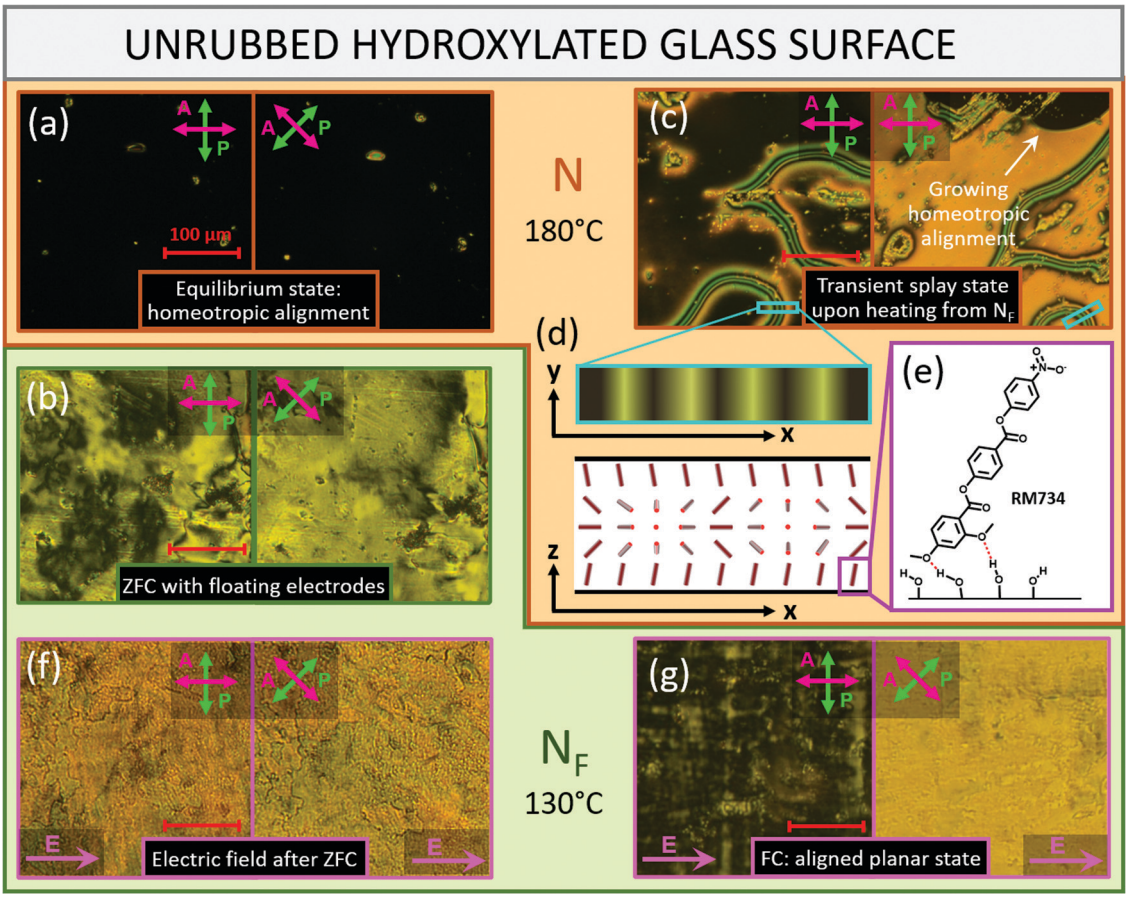

Fig. 5 Polarized transmission optical microscopy images of 18 μm thick RM734-filled cells having hydroxylated glass surfaces. Arrows: analyzer (***A***), polarizer (***P***), electric field (***E***). Shadings: nematic phase (orange), ferroelectric nematic phase (green). (a) Homeotropic alignment is revealed by isotropic refractive index. (b) As T is lowered the homeotropic order is disrupted and the cell adopts a random planar alignment with no detectable favorite direction. (c) When T is increased again, the cells adopt a transient splayed state exhibiting colored patten and 2π splay-bend lines, whose structure is sketched in (d). The splayed state shows a preferential alignment in the loading flow direction, indicating a permanent tilt in the surface-contacting RM734 molecules, possibly reflecting their pattern of H-bonding anchoring (e). In a few seconds, the homeotropic alignment is nucleated and develops filling the whole cell. Electric field effects on N_F phase (pink frames). (f) Application of electric fields up to 20 V cm^{-1} modifies the texture of ZFC cells (b) leading to a pattern which cannot be extinguished by cell rotation, while field cooling from the N_F phase (g) yields good alignment ($E = 7.5$ V cm^{-1}). The value of the scale bar is indicated in the first panel.

showed a transient homeotropic alignment near the isotropic to nematic transition, quickly yielding to stable planar order,[11] a behaviour understood in terms of dipolar interactions with the surface. As the effect of hydroxylation is to increase the number of –OH groups on the glass surfaces, we argue that the homeotropic alignment we observe could be a consequence of H-bonding between hydrogen atoms on the surfaces and the oxygen atoms of the RM734 molecules, as sketched in Fig. 5e.

As the homeotropic cell is cooled into the N_F phase, the perpendicular alignment disrupts, leading to a disordered planar texture which, for the largest part, cannot be locally extinguished by rotating the cell in between crossed polarizers (Fig. 5b and video S5, ESI†). This indicates that the surface provides a local planar orientation strong enough to withstand the elastic torque arising from the conflicting anchoring orientations. We understand the homeotropic (in N) to planar (in N_F) anchoring transition as intimately connected with the nature of the N_F phase: as the polar ordering appears, the homeotropic anchoring becomes incompatible both because of the large energetic cost in sustaining the huge polarization surface charge density and because the H-bond-mediated surface anchoring is itself polar, directed outward from the cell, and thus opposite in the two surfaces.

When the N_F is heated back to the N phase with a slow heating rate, the homeotropic state is recovered. However, for fast rates, a transient nematic pseudo-planar uniform ordering is observed (Fig. 5c and video S6, ESI†), which turns into homeotropic within a few seconds. This transient configuration is preferentially aligned in the cell loading direction and displays colored textures, an indication that the phase retard between polarizations is only a few wavelengths long, *i.e.* that the planar orientation of the nematic is effectively smaller than the physical thickness of the cell. We understand this texture as reflecting the splayed state whose structure is sketched in Fig. 5d. Its preferred alignment along the loading direction suggests the existence of a permanent tilt of the LC molecules on the confining surfaces, possibly reflecting the pattern of H-bond anchoring.

The application of in-plane electric fields in the N_F phase produces a polar response much weaker than for the other surfaces here considered, giving rise to a highly inhomogeneous texture which is different from the one in the absence of a field (in Fig. 5b) and that cannot be extinguished, not even locally, by cell rotation between cross polarizers, indicating a locally twisted structure. This behavior is observed for both positive and negative fields up to 20 V cm^{-1} (Fig. 5f) and indicates that the random planar anchoring adopted in the N_F phase is strong. On the contrary, FC produces well aligned planar states as shown in Fig. 5g for $E = 7.5$ V cm^{-1} in both field directions. The alignment is lost as the field is removed and the cell returns to the random planar alignment of Fig. 5b.

Discussion

Taken all together, the body of observations here presented demonstrates that the degree of surface coupling affects the behavior of RM734 to a great extent, each surface treatment leading to different textures, defect structures, field response, as summarized in Table 1.

Fluorolink-coating results in planar alignment with very low angular coupling, leading to good planar alignment of the N phase along the loading direction, peculiar domain walls and a totally symmetric and high responsivity to electric fields. Moreover, the field-induced alignment is stabilized upon grounding the electrodes. Teflon-rubbed glass plates are also planar, but characterized by a strong directional coupling, giving rise to good uniform planar alignment in both N and N_F phases and to a strongly polar response to external electric fields. The homogeneous alignment induced by rubbing is strong enough to be stable once the field is removed. In between these two surface treatments, silanized glasses also exhibit a planar polar electric field response which however is not stable under field removal. Hydroxylated glass plates give rise to a yet different behavior, with a very marked anchoring transition, that involves the whole cell alignment, as the bulk

Table 1 Summary of the behavior of RM734 for the four different aligning surfaces: LC textures in N and NF phases, response to the external electric field after ZFC and upon FC and stability of the alignment after field removal

Confining surfaces	N Phase (180 °C)	N_F Phase (130 °C)	*E*-Field response after zero field cooling	*E*-Field response upon field cooling	Stability of alignment after field removal
Rubbed silanized glass	Planar alignment along rubbing	Strong quadrupolar alignment along rubbing with preferential polarity	Asymmetric response: uniform polar alignment with $E \leq -1$ V cm^{-1} and $E \geq 5$ V cm^{-1}	Asymmetric polar response similar to zero field cooling.	Not stable
Rubbed Teflon surface	Planar alignment along rubbing	Strong quadrupolar alignment along rubbing with strong preferential polarity	Asymmetric response: uniform polar alignment with $E \leq -1$ V cm^{-1}; no polar alignment observed up to $E = 10$ V cm^{-1}	Asymmetric polar response similar to zero field cooling.	Stable
Unrubbed Fluorolink surface	Degenerate planar alignment: director freely slides on surfaces	Degenerate planar alignment	Symmetric response: uniform polar alignment for $E > 0.5$ V cm^{-1}	Symmetric polar response similar to zero field cooling.	Stable upon grounding electrodes
Unrubbed hydroxylated glass	Homeotropic anchoring	Strong local random polar anchoring	Weak symmetric response. Non-uniform twisted texture up to $E = 20$ V cm^{-1}	Symmetric polar response.	Not stable

polar ordering develops. Such a variety of observations demonstrate that the polar ordering of the N_F phase affects the interaction with the confining surfaces and that, at the same time, the structures adopted by the LC to accommodate the constraints and peculiar energetics of the N_F phase depends on the nature of the confining surfaces themselves. In the case of the two rubbed surfaces, the orientation of preferred polarization is vectorially unidirectional, which gives rise to a uniform bulk polarization and can thus be considered as a surface poling. In-plane electric field of a few V cm^{-1} can thus be used to switch the cell between a uniform and twisted structure, easily converted in bright and dark states, as shown, for a Teflon cell, in ESI,† video S7. Weak coupling to the surfaces allows instead a total π rotation of both the bulk and the surface polarizations under an extremely small external electric field, which also could be exploited for switching by using two electric field directions.

Conclusions

We explored the surface alignment of RM734 and of its ferroelectric nematic phase by testing different rubbed and unrubbed substrates. We observed a diversity of effects depending on the nature and on the treatment of the confining surfaces, all associated to the polar symmetry breaking of the N_F phase. The degree of coupling of RM734 molecules to the specific substrates affects the LC behavior and its response to weak external electric fields, giving rise to N_F phases with different degrees of ordering, and to symmetric or asymmetric field-induced alignment. The nature of the alignment, the domains observed in the N_F phase upon field cooling and zero field cooling are also dependent on the confining surfaces used and the LC distortions underlying them are discussed in the text for each of the four cases considered.

According to our results, the polar ordering of the N_F phase affects the interaction of RM734 with the bounding surfaces, which is a key aspect of nematic LC science and applications. Our results demonstrate that structuring of the vectorial orientation distribution of a 3D volume of polar molecules can be achieved by controlling the polarity of its 2D bounding surfaces.

Conflicts of interest

The authors report no conflicts of interest.

Acknowledgements

F. C., G. N. and T. B. acknowledge support by a PRIN2017 project from Ministero dell'Istruzione dell'Università e della Ricerca (ID 2017Z55KCW). E. K., D. M. W. and N. A. C. acknowledge support by a 3,4, Grant No. and National Science Foundation Grants (DMR 1420736, DMR 1710711 and DMR 200517).

Notes and references

1 R. J. Mandle, S. J. Cowling and J. W. Goodby, *Phys. Chem. Chem. Phys.*, 2017, **19**, 11429–11435.
2 A. Mertelj, L. Cmok, N. Sebastian, R. J. Mandle, R. R. Parker, A. C. Whitwood, J. W. Goodby and M. Copic, *Phys. Rev. X*, 2018, **8**, 041025.
3 H. Nishikawa, K. Shiroshita, H. Higuchi, Y. Okumura, Y. Haseba, S. Yamamoto, K. Sago and H. Kikuchi, *Adv. Mater.*, 2017, **29**, 1702354.
4 N. Sebastian, L. Cmok, R. J. Mandle, M. Rosario de la Fuente, I. Drevenšek Olenik, M. Čopič and A. Mertelj, *Phys. Rev. Lett.*, 2020, **124**, 037801.
5 X. Chen, E. Korblova, D. Dong, X. Wei, R. Shao, L. Radzihovsky, M. Glaser, J. Maclennan, D. Bedrov, D. Walba and N. A. Clark, *Proc. Natl. Acad. Sci. U. S. A.*, 2020, **117**, 14021–14031.
6 N. Sebastián, R. Mandle, A. Petelin, A. Eremin and A. Mertelj, arXiv Prepr. arXiv2103.10215.
7 X. Chen, E. Korblova, M. A. Glaser, J. E. Maclennan, D. M. Walba and N. A. Clark, arXiv Prepr. arXiv2012.15335.
8 J. Cognard, *Alignment of Nematic Liquid Crystals and Their Mixtures*, Gordon and Breach Science Publishers, 1982 ISBN 9780677059051.
9 J. C. Wittmann and P. Smith, *Nature*, 1991, **352**, 414–417.
10 P. Hubert, H. Dreyfus, D. Guillon and Y. Galerne, *J. Phys. II*, 1995, **5**, 1371–1383.
11 Y. Kim, M. Lee, H. S. Wang and K. Song, *Liq. Crystallogr.*, 2018, **45**, 757–764.